

Magnetic transition and spin dynamics in the triangular Heisenberg antiferromagnet α -KCrO₂

F. Xiao,¹ T. Lancaster,¹ P.J. Baker,² F.L. Pratt,² S.J. Blundell,³ J.S. Möller,³ N.Z. Ali,⁴ and M. Jansen⁴

¹*Durham University, Department of Physics, South Road, Durham, DH1 3LE, UK*

²*ISIS Pulsed Neutron and Muon Facility, STFC Rutherford Appleton Laboratory, Harwell Oxford, Didcot, OX11 0QX, UK*

³*University of Oxford, Department of Physics, Clarendon Laboratory, Parks Road, Oxford, OX1 3PU, UK*

⁴*Max-Planck-Institut für Festkörperforschung, Heisenbergstr. 1, 70569 Stuttgart, Germany*

(Dated: September 10, 2018)

We present the results of muon-spin relaxation measurements on the triangular lattice Heisenberg antiferromagnet α -KCrO₂. We observe sharp changes in behaviour at an ordering temperature of $T_c = 23$ K, with an additional broad feature in the muon-spin relaxation rate evident at $T = 13$ K, both of which correspond to features in the magnetic contribution to the heat capacity. This behaviour is distinct from both the Li- and Na- containing members of the series. These data may be qualitatively described with the established theoretical predictions for the underlying spin system.

PACS numbers: 75.10.Jm, 76.75.+i, 75.40.Cx

The geometrical frustration of antiferromagnetic (AFM) interactions continues to be important as a route to creating exotic quantum mechanical ground states including various flavours of quantum spin liquid^{1,2}. Frustration most obviously occurs for antiferromagnetically coupled spins on a triangular lattice but, until recently, there have been relatively few examples of materials well described by a model of Heisenberg spins on such a lattice. In this context the series $A\text{CrO}_2$ (where $A = \text{Li}, \text{Na}, \text{K}$) is of interest as its members comprise well-decoupled, highly ideal, triangular planes containing isotropic spins. While the members of the series with $A = \text{Li}$ ³⁻⁹ and Na ^{3-5,10,11} have been well studied, the material KCrO_2 , which has the best-separated triangular layers and might be expected to best approximate the model, has previously proved difficult to stabilise chemically and has been the subject of less experimental work^{3,4,12}. However, it was recently demonstrated¹³ that KCrO_2 may be reliably synthesized in two different polymorphs, the α - and β -phases, allowing the opportunity for renewed study. Muon-spin relaxation (μ^+ SR) has proven particularly useful in probing both the NaCrO_2 ¹¹ and LiCrO_2 ^{8,9} materials, suggesting unusual spin relaxation spectra in both systems below their respective short- or long-range ordering temperatures, with an exotic fluctuating regime reported well below the short-range ordering temperature T_c in NaCrO_2 , which has better separated layers than LiCrO_2 . Here we present the results of muon-spin relaxation measurements on α -phase KCrO_2 (α -KCrO₂). We find that the fluctuation spectrum in this compound, while showing features that are superficially similar to both the Na- and Li- containing materials, appears to be distinct and unusual. Moreover, although we find that α -KCrO₂ may be described qualitatively within the framework of two different theoretical approaches, it does not seem to admit a quantitative description consistent with either of them.

The structure of the $A\text{CrO}_2$ series comprises well separated triangular planes of $S = 3/2$ Cr^{3+} ions stacking in

an $ABCABC$ sequence with $R\bar{3}m$ symmetry. The separation of the triangular sheets ($1/3$ of the lattice constant c) is found to vary from 4.81 Å for $A = \text{Li}$ to 5.96 Å for $A = \text{K}$, leading us to expect that the potassium-containing material will possess the most magnetically isolated two-dimensional layers. Electron spin resonance measurements on LiCrO_2 and NaCrO_2 ^{5,10} indicate very small single-ion anisotropy, suggesting a strong Heisenberg character for the spins. The structural and magnetic parameters of the members of the series are summarized in Table I. Below $T_N = 62$ K, LiCrO_2 undergoes a transition to a phase of long-range magnetic order (LRO), adopting a 120° magnetic structure⁶ with a suggestion of AFM coupling between layers⁷. Short-range magnetic order (SRO) has been proposed to occur in NaCrO_2 below $T_c = 41$ K. No magnetic Bragg peaks (indicative of LRO) were observed in α -KCrO₂ down to 5 K, but SRO was originally suggested to occur at $T_c = 26$ K on the strength of a diffuse neutron scattering peak⁴. The transition is also confirmed by the more recent heat capacity measurement where a peak is observed at 23 K and by magnetic susceptibility¹³ (where the extracted Fisher heat capacity¹⁴ shows a relatively sharp peak at 24 K). Previous μ^+ SR measurements on the Li⁸ and Na-containing¹¹ materials revealed quite different behaviour in the muon-spin relaxation rate close to the respective ordering temperatures. In LiCrO_2 there is a sharp peak in the relaxation rate at $0.9T_N$. This contrasts with the behaviour of the more two-dimensional NaCrO_2 where the relaxation rate shows a far broader peak, with a maximum at $0.75T_c$. This unusual behavior was justified by considering the nature of the fluctuations in triangular lattice antiferromagnets. It was suggested that NaCrO_2 has an exotic, extended fluctuating regime, with a slow freeze-out of fluctuations below 41 K rather than a conventional ordering transition. It was speculated that this may relate to Z_2 topological defects that have been predicted to occur in the spectrum of the triangular lattice. In contrast, the state of affairs in the more three-

	LiCrO ₂	NaCrO ₂	KCrO ₂
a (Å)	2.898	2.975	3.042
c (Å)	14.423	15.968	17.888
J (K) ^a	78	40	24
θ_{CW} (K)	-620 ⁴ , -700 ³	-290 ³	-160 ³ , -220 ¹³
T_c (K)	62 ^{4,18}	41 ^{4,11}	26 ⁴ , 23 ¹³

^aRef 3 uses the Hamiltonian $-2J\sum_{ij}\mathbf{S}_i\cdot\mathbf{S}_j$ and we use the Hamiltonian $-J\sum_{ij}\mathbf{S}_i\cdot\mathbf{S}_j$, therefore the values of J reported in Ref 3 are doubled in the table for consistency.

TABLE I: Structural and magnetic parameters for compounds in the $ACrO_2$ series ($A = \text{Li, Na, K}$). The cell parameters a and c are from Ref. 4 and the exchange strengths J are from Ref. 3. θ_{CW} is the Curie-Weiss constant derived from the magnetic susceptibility fit.

dimensional LiCrO₂ leads to something closer to the expected behavior of a relaxation rate peaked at T_N .

In a μ^+ SR experiment¹⁵ spin polarized muons are implanted into the sample. The quantity of interest is the angular asymmetry of the decay positrons, $A(t)$, which is proportional to the spin polarization of the muon ensemble. Zero-field muon-spin relaxation (ZF μ^+ SR) measurements were made on a polycrystalline sample of α -KCrO₂ using the EMU spectrometer at the ISIS facility, UK. A sample of α -phase KCrO₂ was prepared as previously described¹³. It was packed, under glove-box conditions, inside a Ti-foil packet (foil thickness 25 μm) and sealed in an air-tight Ti sample holder, which was mounted inside a ⁴He cryostat. The measurements described here were made in the temperature range $1.5 \leq T \leq 200$ K. After the measurements were completed the sample was heated above 500 K in an attempt to detect a transition to the β phase, which we were unable to stabilize.

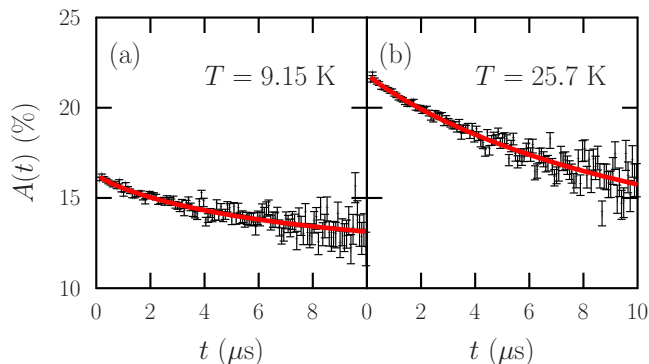


FIG. 1: (Color online.) Example $A(t)$ spectra of polycrystalline α -KCrO₂ at (a) 9.15 K and (b) 25.7 K. Solid lines (red) represent the fit to Eq. (1).

Example ZF μ^+ SR spectra are shown in Fig. 1. Below 23 K we observe a loss of asymmetry in the signal with a transition region $20 \lesssim T \lesssim 23$ K. This is due to the time

resolution limit of the ISIS muon pulse, which prevents the observation of features with rate $\gtrsim 10$ MHz. The loss of asymmetry demonstrates the presence of large, slowly fluctuating moments (see below) which depolarize those muon spin components perpendicular to the local magnetic field (expected to be 2/3 of the total in a powder sample¹⁶). Although it is not possible to tell whether this results from a state of static LRO or SRO on the basis of these measurements, the absence of magnetic Bragg peaks and the fact that the layer separation is greater than for NaCrO₂ where SRO is thought to occur, leads us to tentatively assign T_c as a short-range ordering temperature.

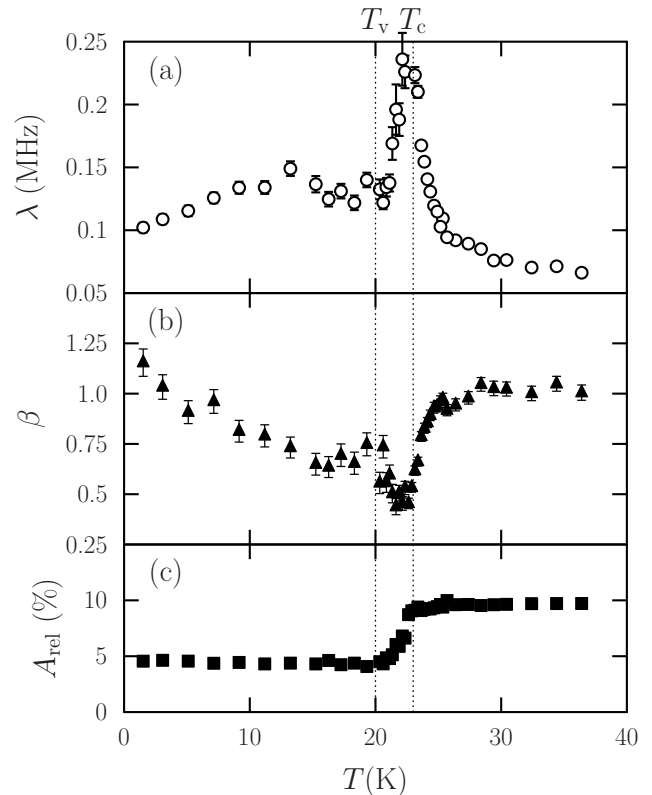


FIG. 2: Evolution of the parameters from Eq. (1) with temperature. Sharp features are observed at 22.6(5) K along with a broad maximum in λ centred on 13 K. T_c is identified from heat capacity peak and T_v is defined in the discussion (see main text).

In order to compare to previous muon measurements on similar triangular materials^{8,11,17}, the muon spectra were fitted to a model of stretched exponential decay with a background contribution:

$$A(t) = A_{\text{rel}}e^{-(\lambda t)^\beta} + A_{\text{bg}}, \quad (1)$$

where A_{rel} represents the amplitude of the relaxing component, λ is the relaxation rate and A_{bg} accounts for the constant background contribution from muons stopping in the sample holder or cryostat tails. The values of λ , β and A_{rel} obtained from the fit are plotted against

temperature in Fig. 2. All three parameters show distinct changes at 22.6(5) K, in agreement with heat capacity measurements¹³ where a sharp peak was observed at $T_c = 23$ K. In addition to the sharp peak in λ , whose rapid decrease levels off below 20 K, the relaxation rate also shows a broad maximum near 13 K, similar to that observed in NaCrO_2 ¹¹.

The relaxation rate λ in Eq. (1) is expected to vary with the width of the local magnetic field distribution Δ and correlation time τ according to $\lambda \propto \Delta^2 \tau$, and therefore the peak in λ is suggestive of a transition to a regime of large, slowly fluctuating moments as the temperature approaches T_c .

The muon-spin relaxation rates for all three compounds in the $A\text{CrO}_2$ family are plotted in Fig. 3 with normalized x -axis. For $\alpha\text{-KCrO}_2$, the maximum in λ occurs at 22.6(5) K and we take $T_c = 23$ K from the heat capacity peak. The relaxation rate for $\alpha\text{-KCrO}_2$ is noticeably smaller than the Li- and Na- compounds, pointing to significantly smaller moments or to shorter fluctuation times. For LiCrO_2 , the sharp peak (corresponding to 3D LRO) occurs a few Kelvin below T_N . NaCrO_2 shows no features close to T_c , but instead we see a broad peak below the critical temperature with the maximum centred on $0.75T_c$. Our measurements on $\alpha\text{-KCrO}_2$, superficially seem to show a combination of both features: not only a sharp peak corresponding to an ordering transition very close to $T_c = 23$ K, but also a very broad shoulder with a maximum centred on $0.57T_c$.

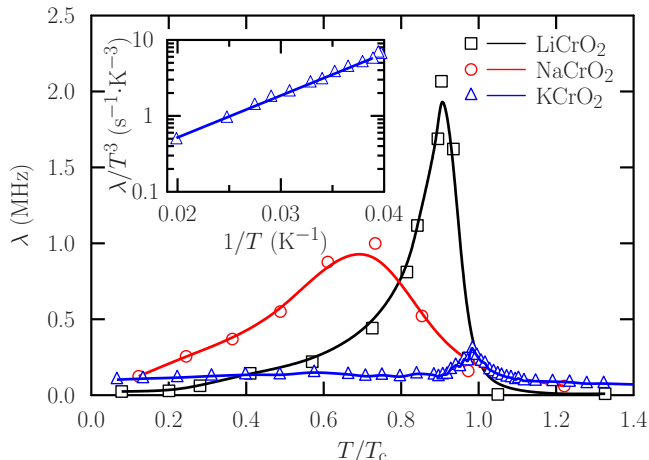


FIG. 3: (Color online.) Comparison of relaxation rates for materials in the series $A\text{CrO}_2$ with $A = \text{Li}, \text{Na}$ and K . The solid lines are a guide to the eye. The peak of $\alpha\text{-KCrO}_2$ appears to be located at a value slightly less than 1, this is due to the experimental uncertainty (we take $T_c = 23$ K from the heat capacity peak for $\alpha\text{-KCrO}_2$). Inset: Dependence of λ/T^3 on inverse temperature $1/T$ for $\alpha\text{-KCrO}_2$. The solid line represents the fit to Eq. (2) for $T > T_c$ and the slope in this semi-log plot corresponds to $T_0/\ln 10$.

It is illuminating to compare the heat capacity results for $\alpha\text{-KCrO}_2$ ¹³ with our muon measurements. The

phonon component of C_p was obtained by fitting the high- T data to a Debye model with $\theta_D = 552$ K. The lattice contribution was then subtracted from the total C_p so only the magnetic heat capacity C_{mag} is plotted in Fig. 4. The low- T region of C_{mag} ($5 \leq T \leq 20$ K) exhibits a T^2 temperature dependence (solid line in Fig. 4), which implies linearly dispersing 2D excitations. This form is also observed for triangular materials showing SRO such as NiGa_2S_4 ¹⁷. In contrast, C_{mag} for LiCrO_2 (which shows LRO) was found to have a T^3 dependence¹⁸ below T_c , consistent with a recent spin-wave theory calculation¹⁹. It is also interesting to note that below 3 K C_{mag} suggests T^2 behaviour but with a different scaling prefactor. In Fig. 4 (inset) the evolution of C_{mag}/T^2 is shown. In addition to the sharp peak at T_c , a broad shoulder is present below T_c with a maximum around 13 K, similar to that observed in the muon relaxation rate. No such shoulder is reported for NaCrO_2 .

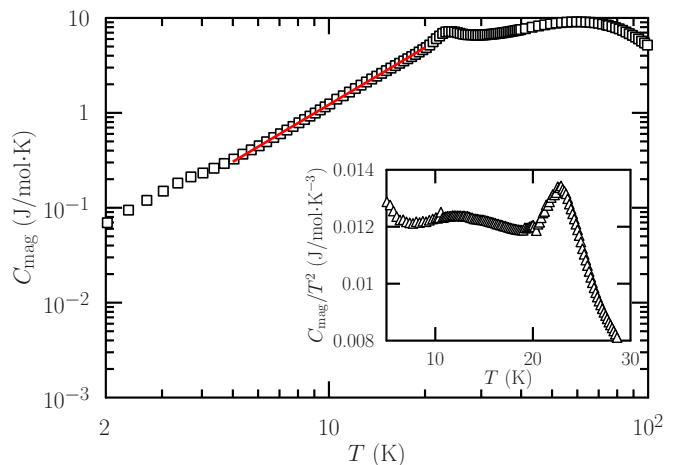


FIG. 4: The magnetic specific heat (C_{mag}) of $\alpha\text{-KCrO}_2$. The solid line is a T^2 fit to the data between 5 K and 20 K. The inset shows C_{mag}/T^2 as a function of temperature.

The results of our $\mu^+\text{SR}$ measurements may be compared against different theoretical descriptions of the triangular lattice AFM Heisenberg model. Above T_c , the spin-wave theory developed by Chubukov, Sachdev, and Senthil (CSS)²⁰ predicts that, for $T \ll 2\pi\rho_s$, the muon relaxation rate follows¹⁷

$$\lambda = G_{\text{CSS}} \left(\frac{N_0 A_0}{\hbar} \right)^2 \frac{\hbar}{\rho_s} \left(\frac{T}{T_0} \right)^3 \exp(T_0/T), \quad (2)$$

where $N_0 A_0$ is a renormalized hyperfine coupling constant, ρ_s is the spin stiffness constant, G_{CSS} is a numerical constant and $T_0 = 4\pi\rho_s$.

By fitting the data above T_c to Eq (2), we are able to obtain T_0 and ρ_s . The fit to the data (Fig. 3 inset) yields $T_0 = 130(2)$ K and $\rho_s = 10.3(2)$ K, which is consistent with the limit $T < 2\pi\rho_s$ for the validity of the model. With the value of ρ_s , the effective exchange coupling J

can then be calculated based on the approximation^{20,21},

$$\frac{\rho_s}{JS^2} = \frac{1 - 0.399/2S}{\sqrt{3}}, \quad (3)$$

where S is the spin quantum number ($3/2$ for α -KCrO₂). The spin-wave exchange strength is found to be $J_{sw} = 9.2$ K. Although the high- T dependence of the relaxation rate is well described by this model, the exchange constant J is much smaller than that obtained from the Curie-Weiss susceptibility fit, where J_θ is found to be 29.3 K¹³ using $|\theta_{SW}| = zJS(S+1)/3$ with $z = 6$, or the value from high temperature series expansion fit obtained in Ref 3, where $J = 24$ K. We therefore find a significant discrepancy between the quantitative values, which is unlike the case of NiGa₂S₄¹⁷ where good agreement was obtained for this model. However it is worth noting that the qualitative agreement with Eq. (2) might suggest that the CSS model captures some of the underlying physical behaviour.

Below T_c , the experimental results are compared to another theoretical description of the triangular lattice system which has been invoked to describe previous μ^+ SR results^{11,17}, known as the spin-gel picture^{22,23}. Here it is suggested that vortex excitations and spin freezing provide two length scales which determine the behaviour: the vortex correlation length ξ_v and spin-wave correlation length ξ_{sw} . The vortex correlation length diverges below a topological critical temperature T_v , where Z_2 vortex excitations undergo a binding transition. However, the spin-wave correlation length remains finite below this temperature, causing the overall effective spin correlation length to remain finite also²³. This T_v is predicted to lie slightly below the peak temperature in the heat capacity, T_{peak} ²². Specifically, quantum Monte Carlo simulations²² have shown that with this model we should expect $T_{peak} = 0.137\theta_{CW}$ and $T_v = 0.123\theta_{CW}$ for classical Heisenberg triangular AFM lattices, where θ_{CW} is the Curie-Weiss constant extracted from fits of the magnetic

susceptibility. This picture may be applied to α -KCrO₂ if we identify T_{peak} with $T_c = 23$ K and T_v with $T = 20$ K, below which the heat capacity C_{mag} follows a T^2 trend due to the dominance of spin-wave excitations and also where the rapid change in muon relaxation rate levels off. Using the relation between T_{peak} , T_v and θ_{CW} , two values of θ_{CW} are obtained $\theta_{CW1} = 23/0.137 = 168$ K and $\theta_{CW2} = 20/0.123 = 163$ K. (In Ref 22 T_v is identified with the rounded shoulder in λ for NaCrO₂. If we adopt the same procedure a value of $\theta_{CW3} = 13/0.123 = 106$ K is derived, which is inconsistent with the value from T_{peak} .) The calculated θ_{CW} values are in reasonable agreement with the $\theta_{CW} = 160$ K measured in Ref 3 but about 25% smaller than the more recent $\theta_{CW} = 220$ K measurement in Ref 13. We note that the latter value of $\theta_{CW} = 220$ K corresponds to the material we measured, where the α -phase was successfully isolated. Given this, and the ambiguity in identifying the features in the data corresponding to T_v it is unclear whether this model is applicable in this case.

In conclusion we have made μ^+ SR measurements on α -phase KCrO₂. The material undergoes a transition, most probably to a region of short-range magnetic order below $T_c = 23$ K and shows evidence for further dynamics below this temperature with a peak seen in the muon-spin relaxation rate and a broad shoulder in the magnetic heat capacity at 13 K. Despite the superficial resemblance to the muon relaxation seen in the Li- and Na- containing members of the series, the features here appear to be unique. Although the behaviour is qualitatively consistent with two established models of the 2D triangular Heisenberg antiferromagnet, namely the CSS spin-wave theory and the spin-gel picture, a fully consistent quantitative description is not obtained with either model.

This work was carried out at the STFC ISIS Facility. We are grateful to STFC for the provision of muon beamtime and to EPSRC (UK) for financial support.

¹ S. Sachdev, *Quantum Phase Transitions* (CUP, Cambridge 2011).
² X-G Wen, *Quantum Field Theory of Many-Body Systems* (OUP, Oxford 2004).
³ C. Delmas, G. Le Flem, C. Fouassier and P. Hagenmuller, *J. Phys. Chem. Solids* **39**, 55 (1978).
⁴ J.L. Soubeyroux, D. Fruchart, C. Delmas and G. Le Flem, *J. Magnetism Magn. Mater.* **14**, 159 (1979).
⁵ A. Angelov *et al.*, *Solid. State. Commun.* **50**, 345 (1984).
⁶ H. Kadowaki, H. Takei and K. Motoya, *J. Phys. Condens. Matter* **7**, 6869 (1995).
⁷ I.I. Mazin, *Phys. Rev. B* **75**, 094407 (2007).
⁸ A. Olariu, P. Mendels, F. Bert, L. K. Alexander, A. V. Mahajan, A.D. Hillier and A. Amato, *Phys. Rev. B* **79**, 224401 (2009).
⁹ Y. Ikedo, J. Sugiyama, K. Mukai, M. Mansson, T. Goko, D. Andreica and A. Amato, *J Phys. Conf. Ser.* **225**, 012016

(2010).
¹⁰ P.R. Elliston *et al.*, *J. Phys. Chem. Solids* **36**, 877 (1975).
¹¹ A. Olariu, P. Mendels, F. Bert, B.G. Ueland, P. Schiffer, R.F. Berger and R.J. Cava, *Phys. Rev. Lett.* **97**, 167203 (2006).
¹² W. Scheld, and R. Hoppe, *Z. Anorg. Allg. Chem.*, **568**, 151 (1989).
¹³ N.Z. Ali, J. Nuss and M. Jansen, *Z. Anorg. Allg. Chem.*, **639**, 241 (2013).
¹⁴ M. E. Fisher, *Phil. Mag.* **7**, 1731 (1962).
¹⁵ S.J. Blundell, *Contemp. Phys.* **40**, 175 (1999).
¹⁶ R.S. Hayano, Y.J. Uemura, J. Imazato, N. Nishida, T. Yamazaki and R. Kubo, *Phys. Rev. B* **20**, 850 (1979).
¹⁷ S. Zhao, P. Dalmass de Reotier, A. Yaouanc, D. E. MacLaughlin, J. M. Mackie, O. O. Bernal, Y. Nambu, T. Higo, and S. Nakatsuji, *Phys. Rev. B* **86**, 064435 (2012).
¹⁸ L.K. Alexander, N. Buttgen, R. Nath, A.V. Mahajan and

- A. Loidl, Phys. Rev. B **76**, 064429 (2007).
- ¹⁹ A. Du, G.Z. Wei and J. Li, Phys. Status Solidi B **234**, 636 (2002).
- ²⁰ A. V. Chubukov, S. Sachdev, and T. Senthil, J. Phys.: Condens. Matter **6**, 8891 (1994).
- ²¹ P. Lecheminant, B. Bernu, C. Lhuillier, and L. Pierre, Phys. Rev. B **52**, 9162 (1995).
- ²² H. Kawamura, A. Yamamoto and T. Okubo, J. Phys. Soc. Jpn. **79**, 023701 (2010).
- ²³ H. Kawamura, J Phys. Conf. Ser. **320** 012002 (2011).